Am J Physiol Heart Circ Physiol 305: H1781–H1789, 2013.
First published October 11, 2013; doi:10.1152/ajpheart.00657.2013.

Discharge of RVLM vasomotor neurons is not increased in anesthetized angiotensin II-salt hypertensive rats

Gustavo R. Pedrino,[1] Alfredo S. Calderon,[2] Mary Ann Andrade,[2] Sergio L. Cravo,[3] and Glenn M. Toney[2]

[1]*Department of Physiological Science, Universidade Federal de Goiás, Goiânia, Brazil;* [2]*Department of Physiology and Center for Biomedical Neuroscience, University of Texas Health Science Center at San Antonio, San Antonio, Texas; and* [3]*Department of Physiology, Universidade Federal de São Paulo, São Paulo, Brazil*

Submitted 27 August 2013; accepted in final form 9 October 2013

Pedrino GR, Calderon AS, Andrade MA, Cravo SL, Toney GM. Discharge of RVLM vasomotor neurons is not increased in anesthetized angiotensin II-salt hypertensive rats. *Am J Physiol Heart Circ Physiol* 305: H1781–H1789, 2013. First published October 11, 2013; doi:10.1152/ajpheart.00657.2013.—Neurons of the rostral ventrolateral medulla (RVLM) are critical for generating and regulating sympathetic nerve activity (SNA). Systemic administration of ANG II combined with a high-salt diet induces hypertension that is postulated to involve elevated SNA. However, a functional role for RVLM vasomotor neurons in ANG II-salt hypertension has not been established. Here we tested the hypothesis that RVLM vasomotor neurons have exaggerated resting discharge in rats with ANG II-salt hypertension. Rats in the hypertensive (HT) group consumed a high-salt (2% NaCl) diet and received an infusion of ANG II (150 ng·kg^{-1}·min^{-1} sc) for 14 days. Rats in the normotensive (NT) group consumed a normal salt (0.4% NaCl) diet and were infused with normal saline. Telemetric recordings in conscious rats revealed that mean arterial pressure (MAP) was significantly increased in HT compared with NT rats ($P < 0.001$). Under anesthesia (urethane/chloralose), MAP remained elevated in HT compared with NT rats ($P < 0.01$). Extracellular single unit recordings in HT ($n = 28$) and NT ($n = 22$) rats revealed that barosensitive RVLM neurons in both groups (HT, 23 cells; NT, 34 cells) had similar cardiac rhythmicity and resting discharge. However, a greater ($P < 0.01$) increase of MAP was needed to silence discharge of neurons in HT (17 cells, 44 ± 5 mmHg) than in NT (28 cells, 29 ± 3 mmHg) rats. Maximum firing rates during arterial baroreceptor unloading were similar across groups. We conclude that heightened resting discharge of sympathoexcitatory RVLM neurons is not required for maintenance of neurogenic ANG II-salt hypertension.

angiotensin II; high-salt diet; hypertension; rostral ventrolateral medulla vasomotor neurons; single unit recording; sympathetic nerve activity

CHRONICALLY ELEVATED ARTERIAL blood pressure (ABP; i.e., hypertension) is among the most common disorders affecting human health and is a leading risk factor for cerebrovascular and ischemic heart disease, cardiac and renal failure, myocardial infarction, and stroke (69). Studies performed in rats have shown that raising the plasma concentration of the hormone ANG II in combination with high salt intake induces hypertension (ANG II-salt hypertension) that is maintained by ongoing sympathetic nerve activity (SNA) (40). The latter is consistent with reports that ANG II-salt hypertension is accompanied by increased plasma norepinephrine concentration (29) and prevented by sympathetic denervation of splanchnic organs by celiac ganglionectomy (30).

Address for reprint requests and other correspondence: G. M. Toney, Dept. of Physiology, Univ. of Texas Health Science Center at San Antonio, 7703 Floyd Curl Dr., San Antonio, TX 78229-3900 (e-mail: toney@uthscsa.edu).

Neuroanatomical studies demonstrate that sympathetic preganglionic neurons in the spinal cord receive direct input from at least five distinct brain regions, including the hypothalamic paraventricular nucleus (PVN), A5 noradrenergic cell group, caudal raphe region, rostral ventromedial medulla, and rostral ventrolateral medulla (RVLM) (27, 52, 62, 63). Of particular importance for the present study are neurons of the RVLM, which play a critical role in both the generation of SNA and its dynamic regulation by visceral afferent reflexes, most notably the arterial baroreceptor reflex (23). Because RVLM neuronal activity is considered an essential determinant of resting ABP (3, 21, 22, 37), experiments were performed to test the hypothesis that sympathoexcitatory RVLM neurons with arterial baroreceptor inhibitable discharge have exaggerated spike frequency in rats with established ANG II-salt hypertension. This possibility is consistent with evidence that ANG II actions drive excitatory oxidative stress in the RVLM of renovascular hypertensive rats (38) and with evidence that intact RVLM function is essential for increased sympathetic tone in spontaneously hypertensive rats (SHR) (11, 19). Additional support for possible enhancement of RVLM vasomotor neuron discharge in ANG II-salt hypertension derives from evidence that elevated salt intake is associated with hyper-reactivity of RVLM control of SNA and ABP (2, 24, 42). The latter is reflected in exaggerated SNA and ABP responses to chemical excitation and inhibition of RVLM (2).

In light of available evidence, we hypothesized that identified sympathoexcitatory RVLM vasomotor neurons will exhibit increased resting discharge in rats with ANG II-salt hypertension compared with normotensive (NT) controls. We further hypothesized that discharge in HT rats would be further enhanced when cardiac rhythmic inhibition was withdrawn by unloading arterial baroreceptors. Determining the contribution of RVLM neurons in mediating ANG II-salt hypertension is an important step toward the goal of identifying molecular and cellular mechanisms that underlie neurogenic contributions to arterial hypertension.

METHODS

Animals. Experiments were performed on 50 male Sprague-Dawley rats (Charles River Laboratories) weighing 350–455 g. Rats were housed in a temperature-controlled room (22°-23°C) on a 14:10 light-dark cycle and had ad libitum access to food and tap water throughout the study. All experimental and surgical procedures were approved by the Institutional Animal Care and Use Committee of the University of Texas Health Science Center at San Antonio and were performed in strict accordance with the National Institutes of Health *Guide for the Care and Use of Laboratory Animals*.

Control rats in the NT group ($n = 22$) consumed a normal salt diet containing 0.4% NaCl. Rats in the hypertensive (HT) group ($n = 28$)

consumed a high-salt diet that contained 2.0% NaCl (Research Diets, New Brunswick, NJ). Nutrient content of normal and high-salt diets was otherwise identical.

Recording mean arterial pressure in conscious rats. Radio telemetry was used to record mean arterial pressure (MAP) and monitor the development of ANG II-salt HT in conscious rats as previously described (12). Briefly, telemetry transmitters (TA11PAC40; Data Sciences, St. Paul, MN) were implanted while rats were anesthetized with isoflurane (2% in 100% O_2). A ventral midline laparotomy was performed, and the transmitter catheter was placed into the abdominal aorta and secured with tissue adhesive (Vetbond; 3M Animal Care Products, St. Paul, MN). Each transmitter was secured to the abdominal wall with suture. Incisions were closed, and animals were placed on a heating pad to maintain body temperature during recovery. Rats each received post-operative antibiotic (G benzathine, 150,000 units/kg sc; AgriLabs, St. Joseph, MO) and analgesic (buprenorphine hydrochloride, 0.05 mg/kg sc; Sigma-Aldrich, St. Louis, MO) treatments and were given 1 wk to recover before recording baseline ABP and heart rate (HR).

Infusion of ANG II or vehicle. After 1 wk of baseline recording, each rat received a subcutaneous osmotic minipump (model 2ML2; Alzet, Cupertino, CA) that delivered either ANG II (Sigma-Aldrich, St. Louis, MO) or vehicle for 14 days. ANG II was delivered at a rate of 150 $ng \cdot kg^{-1} \cdot min^{-1}$. Normotensive control rats were either untreated ($n = 13$) or received an osmotic minipump containing normal saline (0.15 M NaCl) ($n = 9$).

In vivo single-unit recordings. On the day of experiments, rats were anesthetized with isoflurane (3% in O_2) and prepared for single unit extracellular recording as previously described (13, 61, 68). Catheters were inserted into both femoral veins for administration of drugs, and into the right femoral or brachial artery for measurement of ABP. Rats were removed from isoflurane, and anesthesia was maintained with a cocktail of α-chloralose (80 mg/kg iv) and urethane (800 mg/kg iv) (Sigma-Aldrich). Throughout each experiment, supplemental doses of anesthetic were given when needed. After tracheal cannulation, rats were artificially ventilated with oxygen-enriched room air and paralyzed with gallamine triethiodide (25 mg/kg bolus, 7 $mg \cdot kg^{-1} \cdot min^{-1}$; Sigma-Aldrich) in D_5W. End tidal pCO_2 was monitored throughout each experiment and maintained at 40 ± 10 mmHg by adjusting ventilation rate and/or tidal volume. Signals were amplified (5k-10k), band-pass filtered (30–1,000 Hz), and digitized at a frequency of 2,500 Hz using a micro 1401 (Cambridge Electronics Design, Cambridge, UK). Body temperature was maintained at 37 ± 1.0°C with a heated water-circulating pad.

Rats were placed in a stereotaxic head frame, and the skull was leveled between bregma and lambda. A craniotomy was performed to access the RVLM, which was located by mapping the caudal pole of the facial nucleus by recording the antidromic field potential evoked by stimulating (1 mA, 0.1 ms, 1 Hz) the mandibular branch of the facial nerve (CN VII) as previously described (9, 68). Extracellular single-unit recordings were performed using glass microelectrodes filled with isotonic saline containing either 2% Chicago Sky Blue or 5% biotinamide (Vector Laboratories, Burlingame, CA). Electrode tip resistance ranged from 20 to 40 MΩ measured in vivo against a Ag-AgCl reference electrode. Individual RVLM neurons with axons projecting to the spinal cord were identified by antidromic activation. This was achieved by electrical stimulation (1–3 mA, 0.1 ms) of the dorsolateral funiculus at the T2 segment using a concentric bipolar electrode (250 μm od) as previously described (12, 13). Standard criteria were used to verify the antidromic nature of evoked spikes (32). These included having *1*) invariant onset latency, *2*) the ability to faithfully respond to high frequency stimulation, and *3*) the ability of spontaneous action potentials to cancel evoked spikes (i.e., the collision test). To determine whether neurons were baro-inhibitable, ABP was increased with a pressor dose of phenylephrine (10 μg/kg; Sigma-Aldrich) or an inflatable cuff placed suprarenal around the abdominal aorta. All data were digitalized using a micro1401 and analyzed off-line with compatible Spike2 software (v5.15; Cambridge Electronics Design, Cambridge, UK).

Juxtacellular labeling and histology. Upon completion of electrophysiological characterization, a subgroup of neurons was filled with biotinamide using the juxtacellular labeling technique as previously described (53, 67). Briefly, positive polarity current pulses (200 ms duration, 50% duty cycle) of graded amplitude (range: 0.5–6 nA) were delivered through the recording electrode to entrain discharge for 2–10 min while electrostatically ejecting biotinamide from the electrode filling solution. Current pulses were then halted, and recovery of discharge was noted to confirm the viability of entrained neurons. After recovering for 1–4 h, rats underwent transcardiac perfusion with 0.1 M PBS (100 ml) followed by 4% paraformaldehyde (300 ml, pH 7.4) in 0.1 M PBS. Brains were removed and post-fixed in 4% paraformaldehyde for 1 to 2 h, cryoprotected in 30% sucrose-PBS, and sectioned to a thickness of 40 μm. To visualize biotin-filled neurons, free floating sections were incubated with streptavidin conjugated to Alexa Fluor 488 (1:250; Invitrogen, Carlsbad, CA) at room temperature for 3 h. To assess if filled cells belonged to the C1 adrenergic cell group, double labeling was performed for the presence of the enzyme phenylethanolamine-*N*-methyl transferase (PNMT) using a polyclonal antibody (1:1,500; Milipore, Billerica, MA) and Alexa Fluor 594-conjugated to a donkey anti-rabbit IgG (1:300; Invitrogen) (53). Sections were mounted on slides in sequential rostrocaudal order and covered with Prolong Gold Anti-fade Reagent (Invitrogen, Carlsbad, CA). Sections were viewed through a transmission fluorescence microscope (Olympus BX41), and digital images were acquired with a Spot charge-coupled device camera (Diagnostic Instruments).

Data analysis and statistics. MAP and HR responses to ANG II plus high salt intake versus sham treatment were compared by two-way ANOVA (Prism 5.01; GraphPad, La Jolla, CA). Pair-wise comparisons were made with Bonferroni post hoc tests. Group differences in MAP and HR under anesthesia were compared with unpaired *t*-tests. Basal discharge frequency of RVLM neurons was determined from rate meter records (1-s bins) over a representative 5-min data segment while ABP was stable. Unpaired *t*-tests were used to compare group differences in *1)* basal firing rate, *2)* change of MAP needed to silence discharge (ΔMAP Cut-Off), *3*) maximum firing rate during baroreceptor unloading, and *4)* MAP needed to produce the maximum firing rate during baroreceptor unloading. Resting discharge was determined to be cardiac cycle-related by constructing post-ECG R-wave triggered time or phase histograms of unit discharge (Spike2 v5.15; Cambridge Electronics Design). Discharge was considered cardiac rhythmic when a cardiac cycle periodicity was evident in which the maximum and minimum discharge bins deviated by more than 20% from the mean firing rate. Baroreflex function curves relating unit discharge frequency to MAP were constructed by mapping unit discharge into 10-mmHg bins of simultaneously recorded MAP as previously described (50). For illustrative purposes, a Boltzmann sigmoid function was used for curve fitting. Group differences of discharge within specific MAP bins were analyzed by two-way ANOVA. Pair-wise comparisons were made using the Fisher least-significant different post hoc test. Data values throughout the text and figures are expressed as means ± SE.

RESULTS

Effect of ANG II plus salt versus sham treatment on MAP and HR. Figure 1*A* shows summary data of 24-h averaged MAP values recorded by telemetry in sham-treated NT rats ($n = 9$) and HT rats ($n = 15$) treated with ANG II and a high-salt diet. During a 6-day baseline period, MAP was similar in NT (98 ± 1 mmHg) and HT (103 ± 2 mmHg) rats. Heart rate values at baseline (not shown) were also similar across groups (NT, 415 ± 5 beats/min; HT, 408 ± 5 beats/

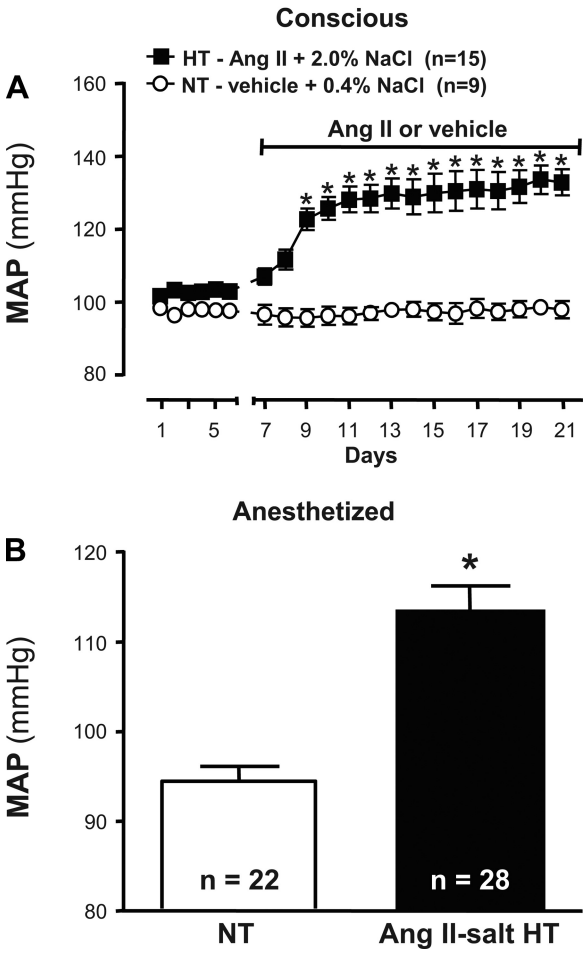

Fig. 1. Effect of ANG II combined with a high-salt diet and sham treatment on mean arterial pressure (MAP) in conscious and anesthetized rats. *A*: baseline values of MAP were recorded by radio telemetry for 6 days before initiating 14 days of subcutaneous infusion of vehicle (normal saline; NT, ○) or ANG II (150 ng·kg^{-1}·min^{-1}; HT, ■). Values of MAP in NT and HT rats were similar at baseline (note that error bars are smaller than symbols). In vehicle-infused NT rats that consumed a normal salt (0.4% NaCl) diet, MAP values throughout the infusion period did not deviate significantly from baseline. In ANG II-infused HT rats that consumed a high-salt (2% NaCl) diet, MAP values increased during the first ~5 days of treatment. Thereafter, MAP remained stably elevated such that values were significantly greater than sham-treated controls (*$P < 0.001$). *B*: during cell recording experiments, resting MAP under urethane/chloralose anesthesia remained significantly elevated in HT (black bar) compared with NT (white bar) rats (*$P < 0.01$).

min). Whereas MAP and HR values in NT rats did not deviate significantly from baseline during the 14 days of vehicle infusion, administration of ANG II in the HT group significantly increased MAP to 123 ± 3 mmHg by *day 3* and to 133 ± 4 mmHg by *day 14* ($P < 0.001$). ANG II infusion had no effect on HR. Figure 1*B* shows that although anesthesia lowered MAP more in HT than NT rats, the average value during RVLM recordings remained significantly greater in ANG II-salt HT rats than NT controls ($P < 0.01$).

Identification and distribution of recorded neurons. Recordings were made from 57 identified RVLM neurons: 34 from NT and 23 from HT rats. Recordings were made posterior to the caudal pole of the facial nucleus, which was located by mapping the antidromic field potential evoked by electrical stimulation of the facial (CN VII) nerve. An example is shown in Fig. 2*A*. Standard criteria were used to classify recorded neurons as subserving sympathoexcitatory vasomotor function. Figure 2*B* shows that neurons were antidromically activated by electrical stimulation of the dorsolateral funiculus at the T1–2 spinal segment on the side ipsilateral to the brain stem recording site. Antidromic spikes exhibited invariant onset latency and the ability to follow high-frequency spinal stimulation (compare top, middle, and bottom traces in Fig. 2*B*, *left*). The average antidromic onset latency was not different between neurons from NT (24 ± 5 ms; $n = 9$) and HT (33 ± 6; $n = 6$) rats. Neurons in the NT and HT group had axonal conduction velocities that averaged 2.0 ± 0.5 m/s and 1.2 ± 0.2 m/s, respectively, indicating that most had unmyelinated axons. Figure 2*B* also shows that evoked spikes underwent time-controlled collision with spontaneous action potentials, thus confirming their antidromic nature. Figure 2*C* shows that neurons were further characterized as sympathoexcitatory by having spontaneous discharge that was strongly inhibited when arterial baroreceptor inputs were activated by raising ABP. Figure 2*D* shows the location of recorded neurons that met the above criteria. They were consistently located within ~700 μm of the caudal pole of the facial nucleus, between 1.7 and 2.1 mm lateral to midline and within ~1.0 mm of the ventral surface of brain. Neurons in NT and HT rats had similar distributions.

Cardiac entrainment of neuronal discharge. Figure 3*A* shows inhibition of spontaneous discharge by raising ABP in an NT and HT rat. Figure 3*B* shows that discharge of the same cells was strongly correlated with the cardiac cycle. Raw data traces from the NT and HT rat show that each recorded cell fired a single spike during each cardiac cycle. Post-R-wave triggered time histograms revealed that these cells fired mostly during the mid-late systolic rise of ABP. Summary data in Fig. 3*C* are reported as phase histograms of spontaneous discharge recorded at resting MAP. Among 34 cells in NT and 23 cells in HT rats, discharge probability was relatively constant during the first ~40% of each cardiac cycle, but fell thereafter in each group to reach a nadir after ~60% of the cardiac cycle had elapsed. There was no significant difference ($F = 0.5885$) in the patterning of cardiac rhythmic discharge across neurons from NT and HT groups. Figure 3*D* shows that despite HT rats having higher resting MAP than NT rats (see Fig. 1*B*), spontaneous discharge frequency was similar ($P = 0.5689$) across groups (NT, 9.5 ± 1.8 spikes/s, $n = 34$; HT, 8.0 ± 1.6 spikes/s, $n = 23$).

Barosensitivity of neuronal discharge. Given that the frequency and cardiac rhythmicity of spontaneous discharge recorded at resting MAP were similar in NT and HT rats, we next determined whether differences in sensitivity to baroreceptor inhibition could be detected. Increasing ABP silenced ongoing discharge of ~82% (28 of 34) of neurons in the NT group and ~74% (17 of 23) of neurons in the HT group. Even among the six neurons from each group whose discharge was not silenced, raising ABP reduced discharge by more than 50%. The increase of MAP needed to silence neuronal discharge was deemed "ΔMAP Cut-Off". An example is shown in Fig. 4*A*. Figure 4*B* shows that the average ΔMAP Cut-Off value was significantly greater ($P < 0.01$) in the ANG II-salt HT group (+44 ± 5 mmHg; $n = 17$) compared with the NT group (+29 ± 3 mmHg; $n = 28$).

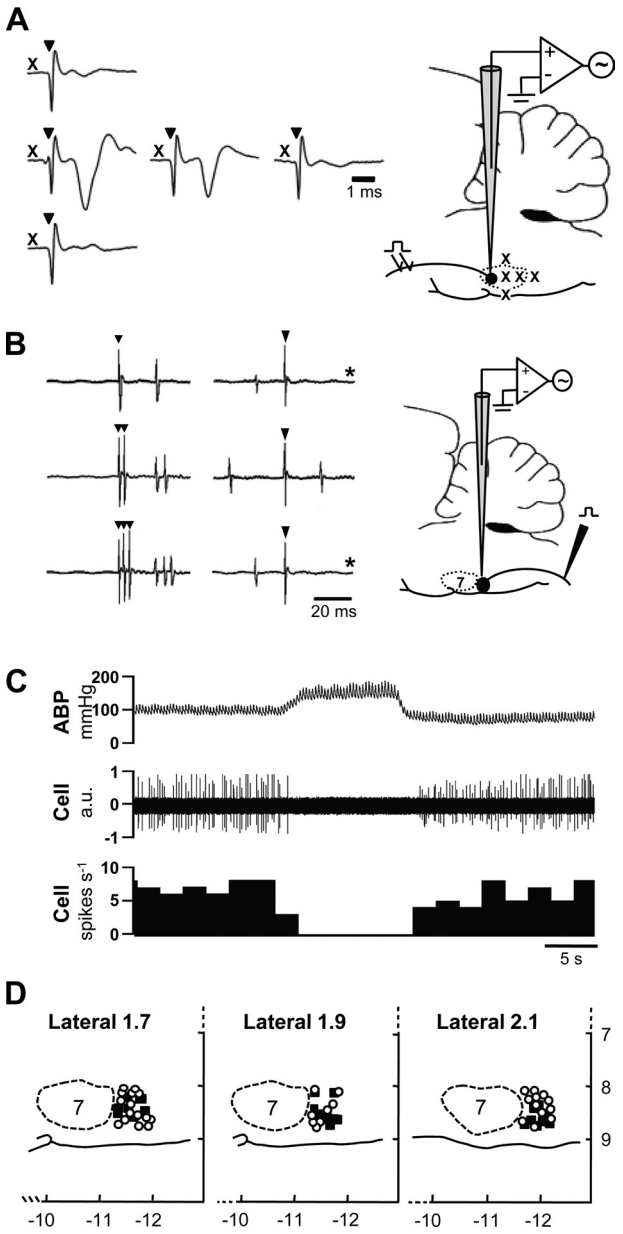

Fig. 2. Identification and distribution of rostral ventrolateral medulla (RVLM) neurons. *A*: RVLM vasomotor neurons are clustered just caudal to the facial nucleus, the caudal pole of which was mapped according to the amplitude of the antidromic field potential evoked by electrical stimulation of the facial nerve (CN VII). X, approximate location of recording sites (see brain stem profile to the right); ▼, stimulus artifacts. Note that the amplitude of the antidromic field potential decays as the recording electrode is moved to more posterior sites within the facial nucleus and disappears when the most caudal boundary of the nucleus is reached. *B*: RVLM vasomotor neurons have axonal projections to spinal cord. Spinally projecting neurons (NT, $n = 9$; HT, $n = 6$) were identified by recording antidromic spikes evoked by stimulation of the T2 spinal segment. The antidromic nature of evoked spikes was confirmed by the consistent onset latency of spikes relative to each stimulus artifact (▼, at *left* and *right*), their ability to follow high frequency (333 Hz) stimulation (middle and lower traces at *left*), and collision with spontaneous action potentials (at *right*; *sweeps where collision occurred). *C*: spontaneous discharge of recorded RVLM neurons was consistently inhibited by raising arterial blood pressure (ABP). *D*: recorded RVLM neurons in NT (○) and HT (■) rats were similarly distributed and consistently located within ~700 μm of the caudal pole of the facial nucleus, 1.7–2.1 mm lateral to midline and within 1.0 mm of the ventral surface of brain. Note that x- and y-axis values are distances (in mm) relative to bregma and brain surface, respectively. AU, arbitrary units.

Among a subgroup of neurons silenced by raising ABP, sodium nitroprusside was used to lower ABP and unload arterial baroreceptors. An example is shown in Fig. 4*C*. Summary data in Fig. 4*D* reveal that the maximum baro-unloaded firing rate was similar in NT (17.4 ± 4.1 spikes/s; $n = 15$) and HT (15.3 ± 4.1 spikes/s; $n = 12$) groups ($P = 0.7227$). The level of MAP needed to achieve maximum baro-unloaded firing rate was also similar ($P = 0.4654$) between groups (NT, 62 ± 3 mmHg; HT, 65 ± 4 mmHg). Figure 4*E* shows summary baroreflex function curves for each group (NT, 34 cells; HT, 21 cells). Note that across a wide range of MAP values, discharge frequency among identified RVLM neurons did not differ significantly across groups. However, discharge of neurons in the HT group did exceed that of neurons in the NT group ($P < 0.05$) at values of MAP that just exceeded baseline (range, 120–150 mmHg).

Chemical phenotyping of recorded neurons. The adrenergic phenotype (C1 or non C1) was determined for a subset of recorded neurons recovered after successful juxtacellular labeling. An example is shown in Fig. 5*A*. Of 19 recovered neurons, three from NT rats and six from ANG II-salt HT rats were PNMT positive and thus were designated C1 cells (Fig. 5*B*, *left*). The remaining 10 cells, four from NT and six from HT rats, did not show detectable PNMT immunoreactivity and were classified as non-C1cells (Fig. 5*B*, *right*). Although there was a trend for non-C1 cells to fire faster than C1 cells in both NT and HT groups, summary data in Fig. 5*C* indicate no significant group differences in discharge of C1 (NT, 5.8 ± 1.6 spikes/s; HT, 6.8 ± 3.5 spikes/s; $P < 0.8838$) and non-C1 (NT, 10.1 ± 1.6 spikes/s; HT, 9.8 ± 2.9 spikes/s; $P = 0.9596$) cells.

DISCUSSION

Studies in animals (14, 16, 18, 23, 68) and humans (18, 20, 51, 57) demonstrate that neurogenic mechanisms contribute to the pathophysiology of arterial hypertension. Despite abundant evidence that neurons of the RVLM are the dominant controllers of vasomotor SNA and cardiovascular function (5, 16, 22, 23, 49, 58, 68), direct evidence that their spontaneous discharge frequency is increased in experimental hypertension is lacking. Here we report that although maintenance of ANG II-salt hypertension depends on ongoing SNA (39, 40), identified RVLM vasomotor neurons in HT rats exhibit only a modest resistance to arterial baroreceptor inhibition with no increase in resting discharge compared with NT controls.

Consistent with previous reports (12, 29, 30, 40, 41, 68), resting MAP and HR in the present study were similar among rats that consumed a high-salt (2% NaCl) and a normal salt (0.4% NaCl) diet. Upon infusion of ANG II, MAP increased rapidly in the high-salt group, reaching a stable level after ~5 days. HR was unchanged as previously reported (12, 29, 30, 40, 41). These temporal patterns are again consistent with previous reports (12, 29, 30, 40, 41, 68) but contrast with vehicle infused/untreated rats in which both MAP and HR remained at the baseline level throughout the 14-day treatment period.

Maintenance of ANG II-salt hypertension critically depends on ongoing SNA. Studies demonstrate that plasma norepinephrine increases along with MAP (29) and that denervation of splanchnic organs by celiac ganglionectomy also prevents the delayed plateau phase of the hypertension (30). Direct evi-

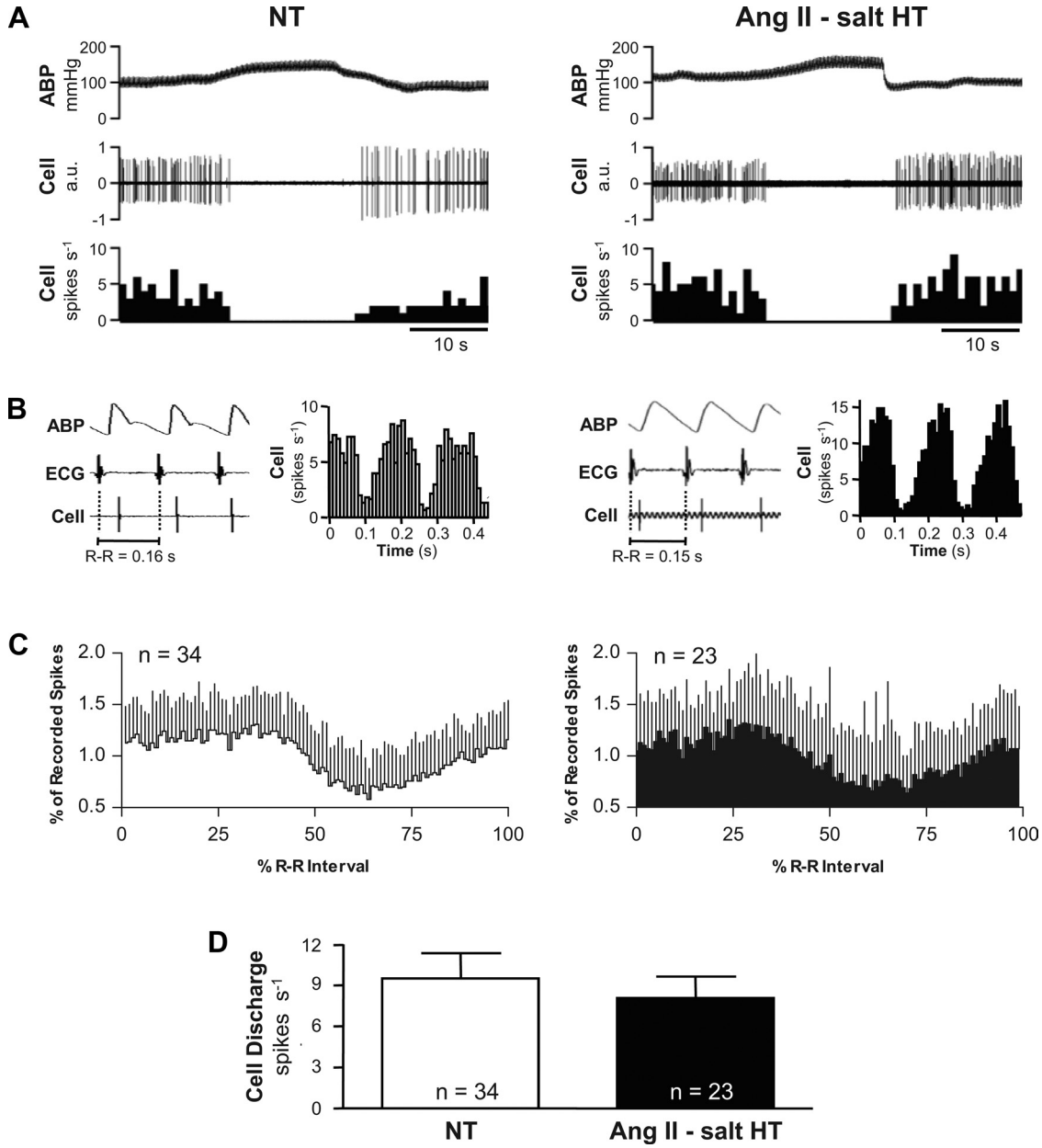

Fig. 3. Barosensitivity and cardiac rhythmicity of RVLM neuronal discharge. *A*: example of the response of a recorded neuron in an NT (*left*) and HT (*right*) rat. Note that in both case discharge was silenced when ABP was raised by inflating an aortic cuff. *B*: example traces of ABP, ECG (lead II), and cell discharge show that neurons in NT (*left*) and HT (*right*) rats fired with a consistent temporal relation to cardiac depolarization (R waves) and pulsatile ABP. R-wave triggered time histograms of unit discharge reveal that spontaneous discharge in the NT (*left*) and HT (*right*) rat was strongly cardiac rhythmic. *C*: summary R-wave triggered phase histograms constructed from 34 cells recorded in NT rats (*left*) and 23 cells recorded in HT rats (*right*). Note that pulse rhythmic baroreceptor inhibition produced a similar magnitude reduction of discharge probability in both groups, with the nadir consistently occurring after ~60% of the cardiac cycle period had elapsed. *D*: summary data reveal that the average resting discharge frequency among identified RVLM vasomotor neurons was similar in cells from NT (white bar) and HT (black bar) rats.

dence that sympathetic outflow to splanchnic organs is increased in ANG II-salt hypertension is lacking (70), but studies have reported that splanchnic vascular resistance is increased (31, 39). Although the latter might not result from elevated splanchnic SNA, it is presumed to be sufficient to support elevated MAP since chronic recordings in conscious rats indicate that renal SNA falls and lumbar SNA is unchanged during development of ANG II-salt hypertension (70). Collectively, evidence suggests that neurogenic mechanisms develop gradually and contribute to maintenance of ANG II-salt hypertension. Importantly, the contribution of SNA to support of ANG II-salt hypertension does not appear to solely reflect increased vascular reactivity to released norepinephrine since interruption of neural activity in specific brain regions selectively blunts the delayed neurogenic phase of the hypertension (41, 43, 44).

Studies document that RVLM vasomotor neurons are located just posterior (within ~700 μm) to the caudal pole of the facial nucleus and have specific characteristics that include monosynaptic excitatory connections to spinal sympathetic

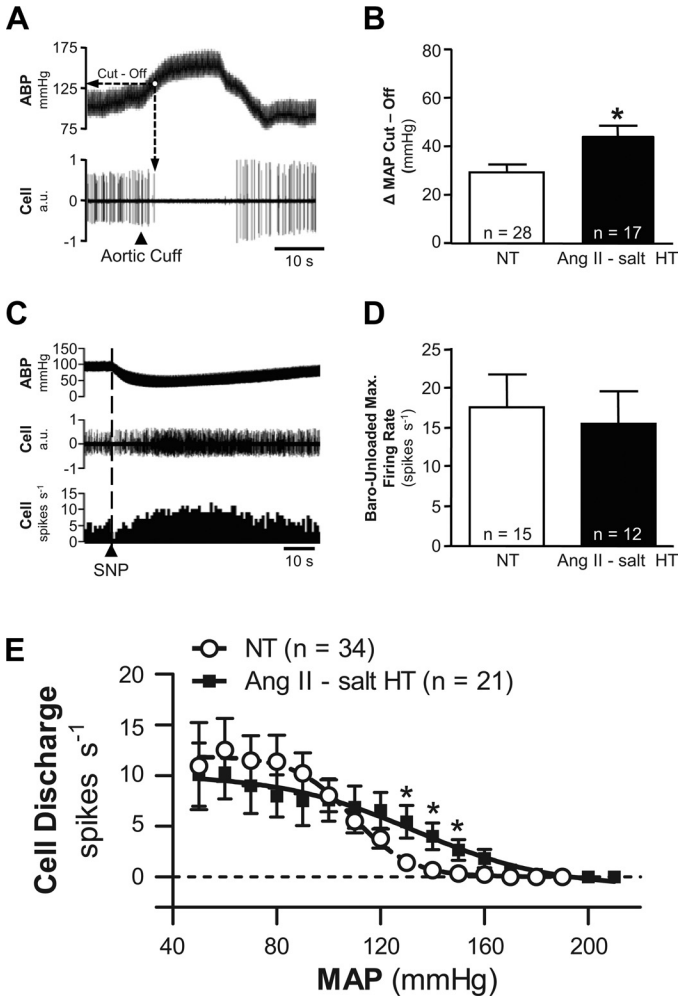

Fig. 4. Comparison of barosensitivity of RVLM neuronal discharge. *A*: example data show that raising ABP by inflation of an aortic cuff led to silencing of discharge. The change of MAP required to silence cell discharge was deemed "ΔMAP Cut-Off." *B*: summary data for 28 neurons from NT rats (white bar) and 17 neurons from HT rats (black bar) indicate that a significantly ($*P < 0.01$) greater increase of MAP was required to fully silence neurons in the HT group. *C*: example traces show that intravenous injection of the vasodilator sodium nitroprusside (SNP) consistently lowered AB and increased discharge of identified RVLM neurons. *D*: summary data of maximum firing rate achieved during SNP-induced unloading of arterial baroreceptors. Note that discharge increased similarly among neurons in NT (white bar) and HT (black bar) rats. *E*: summary baroreflex function curves relating MAP to RVLM discharge frequency. Note that NT (○) and HT (■) groups had similar maximum discharge frequency during baroreceptor unloading and similar minimum discharge frequency when MAP as raised. Neurons in the ANG II-salt HT group showed a significant degree of resistance to baroinhibition across values of MAP ranging from 120 to 150 mmHg.

preganglionic neurons along with cardiac rhythmic and baroreceptor inhibitable spontaneous discharge (9, 10, 37). Neurons recorded in the present study shared these properties. Due to the important role RVLM neurons play in cardiovascular regulation, we hypothesized that their hyperactivity could lead to increased SNA and thereby contribute to maintenance of ANG II-salt hypertension. Consistent with this hypothesis, studies have shown that acute inhibition of RVLM dramatically reduces ABP in several experimental models of hypertension (6, 7, 25, 26, 59). But despite such evidence, a previous study reported that spontaneous discharge frequency of RVLM vasomotor neurons did not differ between NT rats and SHR (64). As in the SHR study, we also found no difference in resting discharge between NT and ANG II-salt HT rats among a similar population of recorded RVLM neurons. Drawing parallels between these two studies is complicated by several factors. First, SHR are an inbred strain used to model essential hypertension. Thus substantial genetic differences between SHR and the Sprague-Dawley rats used in the present study could confound direct comparisons. In addition, whereas recordings in SHR were performed under halothane anesthesia, our rats were anesthetized with a mixture of α-chloralose and urethane. This raises several issues. First and most important is that both anesthetics reduced MAP more in the HT group than in NT controls. Thus anesthesia might have prevented detection of differences in resting discharge that could have existed while rats were conscious. Another issue to consider is that under halothane anesthesia resting discharge of RVLM neurons in both SHR and normotensive Wistar-Kyoto rats was more than twice that reported when other anesthetics are used, including α-chloralose/urethane used in the present study (10, 33, 35, 37). Thus inhibitory and excitatory efficacy of inputs to RVLM in the SHR study could have been compromised, thereby shifting the balance of control in favor of excitation relative to the present study, again confounding direct comparison.

Despite these experimental differences, results of the two studies overall were nevertheless remarkably similar. Both studies indicate that regulation of RVLM neuronal discharge by arterial baroreceptors was mostly intact in HT compared with NT rats. In both studies, the pressor level required to silence neurons was higher in HT rats, indicating that baroreceptor inhibition of these neurons was blunted, but not enough to result in a significant increase of resting discharge at the prevailing level of baseline MAP. Whether attenuation of baroreceptor inhibition was due to reduced mechano-transduction of baroreceptor endings, blunted transmission of baroreceptor inputs, or reduced postsynaptic response to baroreceptor inhibition is not presently known. Certainly a combination of these factors could be involved. It should also be emphasized that because resting MAP was higher in rats with ANG II-salt hypertension, smaller increments were required to raise MAP to specific levels above baseline. Consequently, higher discharge values at elevated MAP in HT rats could simply reflect less recruitment of baroreceptor inputs rather than a specific biological mechanism conferring resistance of RVLM neurons to baroreceptor inhibition.

Whichever the case might be, blunted inhibitory modulation in the present study was apparent only across a narrow range of MAP that just exceeded the resting value under anesthesia. It seems unlikely that this would account for exaggerated SNA that contributes to ANG II-salt hypertension. It should be emphasized, however, that the narrow range of MAP over which significant blunting of baroreflex inhibition was evident in the present study closely overlapped with the level of hypertension recorded by telemetry while rats were conscious. This suggests that inhibitory efficacy of baroreceptor inputs might be selectively blunted in ANG II-salt HT rats at levels of MAP that lie close to the prevailing level of chronic hypertension. Whether this could be a contributing or permissive factor in the development/maintenance of the hypertension or is simply an adaptive or compensatory response to the hyperten-

sion requires further investigation. Although evidence clearly indicates that circulating and brain-derived ANG II are capable of acutely and chronically modifying arterial baroreflex control of SNA in a variety of species (4, 8, 34, 36), studies to date have not documented specific baroreflex alterations (e.g., gain, set point, functional range, etc.) in the same rat model of ANG II-salt hypertension used in the present study. A final consideration is that ANG II-salt hypertension is presumed to rely on a selective increase of splanchnic SNA (30, 39, 40, 70). If this is ultimately proven correct, then it would seem possible that a specific subpopulation of RVLM neurons might exist that selectively supplies exaggerated sympathetic traffic to splanchnic organs in ANG II-salt HT rats. That being the case, then it would seem that we either entirely failed to detect such neurons or that they were not sufficiently enriched within the population of recorded cells to have produced a statistically greater average firing rate in the ANG II-salt HT group compared with controls.

There is substantial evidence that both circulating ANG II and high salt intake strongly influence cardiovascular homeostasis. Circulating ANG II and hypertonic NaCl both activate neurons of the hypothalamic PVN through excitatory projections from the subfornical organ (17, 46, 55, 66) and ventral forebrain (1, 56, 61). Once activated, PVN neurons could increase SNA and ABP through projections to a variety of downstream targets, most notably RVLM vasomotor neurons and spinal sympathetic preganglionic neurons (13, 15, 45, 47, 54, 60, 65). Differentiating between these possibilities requires further investigation, but the present results suggest either that SNA is not elevated in ANG II-salt HT rats or that pathways not involving RVLM could participate. The possibility that RVLM neurons do not drive neurogenic contributions to ANG II-salt hypertension is consistent with their resting discharge being similar among NT and HT rats and with our observation that their maximal discharge during baroreceptor unloading was also similar across groups. During baroreceptor unloading, RVLM neurons are effectively devoid of their dominant source of ongoing inhibition. Under these conditions, their discharge would be expected to most strongly reflect convergent drives descending from ANG II and sodium-sensitive regions of the forebrain and hypothalamus. Yet, even under these conditions, no group difference in RVLM neuronal discharge frequency was detected. We acknowledge that this does not fully eliminate the possibility that excitability/excitatory drive is enhanced among RVLM vasomotor neurons in conscious ANG II-salt HT rats. However, results are consistent with the possibility that RVLM neurons and feed-forward sympathoexcitatory neurons of the forebrain/hypothalamus might operate in parallel in ANG II-salt hypertension such that descending sympathoexcitatory drives largely bypass RVLM. There is evidence to support such a possibility (28, 48), but to our knowledge not in the specific case of neurogenic hypertension.

In sum, results of the present study indicate that combined treatment with systemic ANG II and a high-salt diet does not

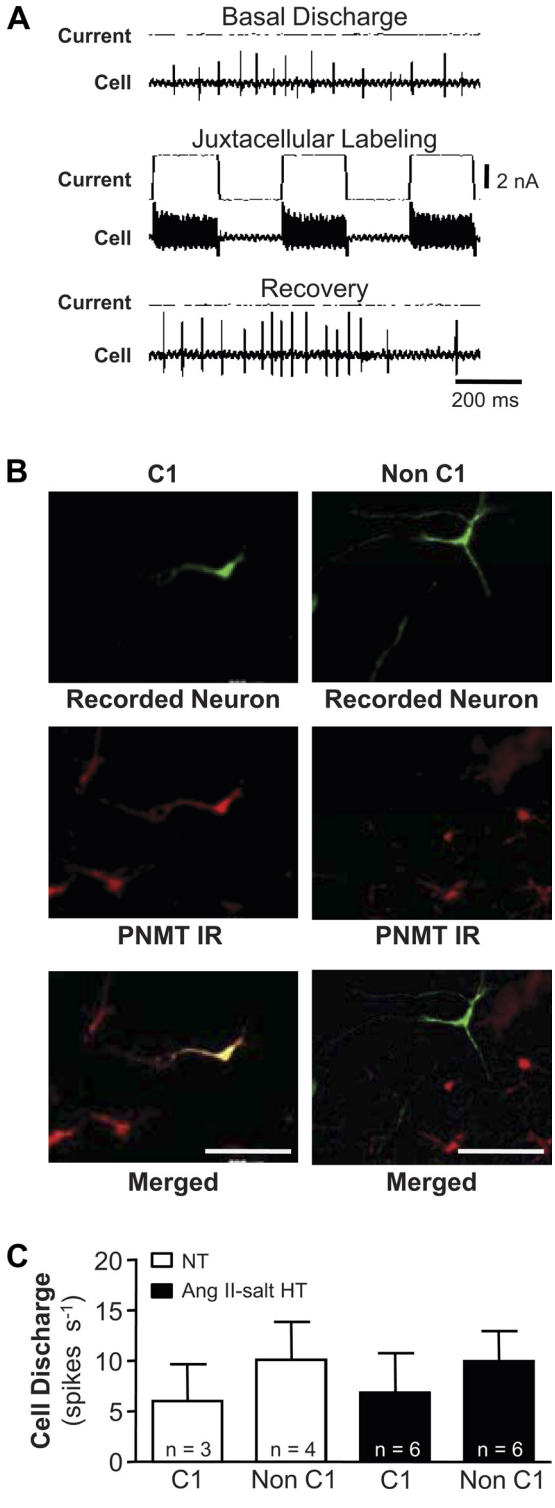

Fig. 5. Neurochemical phenotyping of RVLM neurons. *A*: example traces illustrate the juxtacellular labeling technique. Discharge of a representative RVLM neuron is shown at rest (top traces), during delivery of positive current pulses through the recording electrode to entrain discharge (during which the recorded neuron is filled with biotinamide [middle traces]), and during recovery (bottom traces). *B*: histological processing of brain tissue was performed to recover recorded neurons that were successfully filled with biotinamide using the juxtacellularly labeling technique (at *top*; green). Immunohistochemical processing of the same tissue sections revealed the presence of the epinephrine synthetic enzyme phenylethanolamine-*N*-methyl transferase (PNMT), thereby marking the location of C1 cells (at *middle*; red). Merged images (*bottom*) reveal double-labeled neurons that belong to the C1 cell group (at *left*; yellow) and nondouble labeled neurons that do not (at *right*; green). *C*: summary data show that resting discharge frequencies were similar among C1 and non-C1 neurons from NT and HT rats. IR, immunoreactivity.

change resting discharge frequency of identified RVLM vasomotor neurons. As indicated above, this conclusion must be tempered by the fact that recordings were made in anesthetized rats. Of note, anesthesia lowered resting MAP more in ANG II-salt HT than NT rats, and this could reflect a greater anesthesia-induced reduction of RVLM vasomotor neuron discharge in the HT group. Such an effect could have effectively masked a difference in resting discharge between groups. An argument against anesthesia having a generalized effect to blunt neuronal excitability is that maximal discharge frequency during complete baroreceptor unloading did not differ in NT and HT rats. Our observation that the resting discharge of RVLM vasomotor neurons did not differ among ANG II-salt hypertensive and normotensive rats suggests either that SNA is not elevated in ANG II-salt hypertension or that any increase of SNA that contributes to the hypertension is driven by sympathetic premotor neurons that reside outside of RVLM. In addition, pre- and/or postganglionic sympathetic neurons that lie distal to RVLM could undergo adaptive changes in rats with ANG II-salt hypertension such that they exhibit exaggerated responses to inputs they receive, be they inputs from RVLM or other sympathetic regulatory regions of brain. Consistent with evidence from recordings in SHR (64), we conclude that exaggerated resting discharge of RVLM vasomotor neurons does not contribute to neurogenic ANG II-salt hypertension. Of note, this conclusion appears to extend to both C1 and non-C1 neurons.

ACKNOWLEDGMENTS

We thank Myrna Herrera-Rosales for excellent technical assistance.

GRANTS

This work was supported by National Heart, Lung, and Blood Institute Grant HL-102310 (to G. M. Toney) and Conselho Nacional de Desenvolvimento Científico e Tecnológico (CNPq; No. 477832/2010-5). The funders had no role in the study design, data collection/analysis, decision to publish, or preparation of the manuscript.

DISCLOSURES

No conflicts of interest, financial or otherwise, are declared by the author(s).

AUTHOR CONTRIBUTIONS

Author contributions: G.R.P., S.L.C., and G.M.T. conception and design of research; G.R.P., A.S.C., M.A.A., and G.M.T. performed experiments; G.R.P., A.S.C., M.A.A., and G.M.T. analyzed data; G.R.P., S.L.C., and G.M.T. interpreted results of experiments; G.R.P., A.S.C., M.A.A., and G.M.T. prepared figures; G.R.P. and G.M.T. drafted manuscript; G.R.P., S.L.C., and G.M.T. edited and revised manuscript; G.R.P., A.S.C., M.A.A., S.L.C., and G.M.T. approved final version of manuscript.

REFERENCES

1. **Adams JM, Bardgett ME, Stocker SD.** Ventral lamina terminalis mediates enhanced cardiovascular responses of rostral ventrolateral medulla neurons during increased dietary salt. *Hypertension* 54: 308–314, 2009.
2. **Adams JM, Madden CJ, Sved AF, Stocker SD.** Increased dietary salt enhances sympathoexcitatory and sympathoinhibitory responses from the rostral ventrolateral medulla. *Hypertension* 50: 354–359, 2007.
3. **Barman SM, Gebber GL.** Rostral ventrolateral medullary and caudal medullary raphe neurons with activity correlated to the 10-Hz rhythm in sympathetic nerve discharge. *J Neurophysiol* 68: 1535–1547, 1992.
4. **Barrett CJ, Guild SJ, Ramchandra R, Malpas SC.** Baroreceptor denervation prevents sympathoinhibition during angiotensin II-induced hypertension. *Hypertension* 46: 168–172, 2005.
5. **Beluli DJ, Weaver LC.** Areas of rostral medulla providing tonic control of renal and splenic nerves. *Am J Physiol Heart Circ Physiol* 261: H1687–H1692, 1991.
6. **Bergamaschi C, Campos RR, Schor N, Lopes OU.** Role of the rostral ventrolateral medulla in maintenance of blood pressure in rats with Goldblatt hypertension. *Hypertension* 26: 1117–1120, 1995.
7. **Bergamaschi CT, Campos RR, Lopes OU.** Rostral ventrolateral medulla: a source of sympathetic activation in rats subjected to long-term treatment with L-NAME. *Hypertension* 34: 744–747, 1999.
8. **Brooks VL.** Interactions between angiotensin II and the sympathetic nervous system in the the long-term control of arterial pressure. *Clin Exp Pharmacol Physiol* 24: 83–90, 1997.
9. **Brown DL, Guyenet PG.** Cardiovascular neurons of brain stem with projections to spinal cord. *Am J Physiol Regul Integr Comp Physiol* 247: R1009–R1016, 1984.
10. **Brown DL, Guyenet PG.** Electrophysiological study of cardiovascular neurons in the rostral ventrolateral medulla in rats. *Circ Res* 56: 359–369, 1985.
11. **Chan RK, Chan YS, Wong TM.** Effects of [Sar1, Ile8]-angiotensin II on rostral ventrolateral medulla neurons and blood pressure in spontaneously hypertensive rats. *Neuroscience* 63: 267–277, 1994.
12. **Chen QH, Andrade MA, Calderon AS, Toney GM.** Hypertension induced by angiotensin II and a high salt diet involves reduced SK current and increased excitability of RVLM projecting PVN neurons. *J Neurophysiol* 104: 2329–2337, 2010.
13. **Chen QH, Toney GM.** Identification and characterization of two functionally distinct groups of spinal cord-projecting paraventricular nucleus neurons with sympathetic-related activity. *Neuroscience* 118: 797–807, 2003.
14. **Colombari E, Sato MA, Cravo SL, Bergamaschi CT, Campos RR Jr, Lopes OU.** Role of the medulla oblongata in hypertension. *Hypertension* 38: 549–554, 2001.
15. **Coote JH.** Landmarks in understanding the central nervous control of the cardiovascular system. *Exp Physiol* 92: 3–18, 2007.
16. **Dampney RA, Horiuchi J, Tagawa T, Fontes MA, Potts PD, Polson JW.** Medullary and supramedullary mechanisms regulating sympathetic vasomotor tone. *Acta Physiol Scand* 177: 209–218, 2003.
17. **Dawson CA, Jhamandas JH, Krukoff TL.** Activation by systemic angiotensin II of neurochemically identified neurons in rat hypothalamic paraventricular nucleus. *J Neuroendocrinol* 10: 453–459, 1998.
18. **Esler M, Lambert E, Schlaich M.** Point: chronic activation of the sympathetic nervous system is the dominant contributor to systemic hypertension. *J Appl Physiol* 109: 1996–1998, 2010.
19. **Fink GD.** Long-term sympatho-excitatory effect of angiotensin II: a mechanism of spontaneous and renovascular hypertension. *Clin Exp Pharmacol Physiol* 24: 91–95, 1997.
20. **Grimson KS.** Total thoracic and partial to total lumbar sympathectomy and celiac ganglionectomy in the treatment of hypertension. *Ann Surg* 114: 753–775, 1941.
21. **Guertzenstein PG.** Blood pressure effects obtained by drugs applied to the ventral surface of the brain stem. *J Physiol* 229: 395–408, 1973.
22. **Guertzenstein PG, Silver A.** Fall in blood pressure produced from discrete regions of the ventral surface of the medulla by glycine and lesions. *J Physiol* 242: 489–503, 1974.
23. **Guyenet PG.** The sympathetic control of blood pressure. *Nat Rev Neurosci* 7: 335–346, 2006.
24. **Ito S, Gordon FJ, Sved AF.** Dietary salt intake alters cardiovascular responses evoked from the rostral ventrolateral medulla. *Am J Physiol Regul Integr Comp Physiol* 276: R1600–R1607, 1999.
25. **Ito S, Komatsu K, Tsukamoto K, Sved AF.** Excitatory amino acids in the rostral ventrolateral medulla support blood pressure in spontaneously hypertensive rats. *Hypertension* 35: 413–417, 2000.
26. **Ito S, Komatsu K, Tsukamoto K, Sved AF.** Tonic excitatory input to the rostral ventrolateral medulla in Dahl salt-sensitive rats. *Hypertension* 37: 687–691, 2001.
27. **Jansen AS, Wessendorf MW, Loewy AD.** Transneuronal labeling of CNS neuropeptide and monoamine neurons after pseudorabies virus injections into the stellate ganglion. *Brain Res* 683: 1–24, 1995.
28. **Kiely JM, Gordon FJ.** Role of rostral ventrolateral medulla in centrally mediated pressor responses. *Am J Physiol Heart Circ Physiol* 267: H1549–H1556, 1994.
29. **King AJ, Novotny M, Swain GM, Fink GD.** Whole body norepinephrine kinetics in ANG II-salt hypertension in the rat. *Am J Physiol Regul Integr Comp Physiol* 294: R1262–R1267, 2008.

30. **King AJ, Osborn JW, Fink GD.** Splanchnic circulation is a critical neural target in angiotensin II salt hypertension in rats. *Hypertension* 50: 547–556, 2007.
31. **Kuroki MT, Guzman PA, Fink GD, Osborn JW.** Time-dependent changes in autonomic control of splanchnic vascular resistance and heart rate in ANG II-salt hypertension. *Am J Physiol Heart Circ Physiol* 302: H763–H769, 2012.
32. **Lipski J.** Antidromic activation of neurones as an analytic tool in the study of the central nervous system. *J Neurosci Methods* 4: 1–32, 1981.
33. **Lipski J, Lin J, Teo MY, van WM.** The network vs. pacemaker theory of the activity of RVL presympathetic neurons—a comparison with another putative pacemaker system. *Auton Neurosci* 98: 85–89, 2002.
34. **Lohmeier TE, Dwyer TM, Hildebrandt DA, Irwin ED, Rossing MA, Serdar DJ, Kieval RS.** Influence of prolonged baroreflex activation on arterial pressure in angiotensin hypertension. *Hypertension* 46: 1194–1200, 2005.
35. **McAllen RM.** Central respiratory modulation of subretrofacial bulbospinal neurones in the cat. *J Physiol* 388: 533–545, 1987.
36. **Moretti JL, Burke SL, Davern PJ, Evans RG, Lambert GW, Head GA.** Renal sympathetic activation from long-term low-dose angiotensin II infusion in rabbits. *J Hypertens* 30: 551–560, 2012.
37. **Morrison SF, Milner TA, Reis DJ.** Reticulospinal vasomotor neurons of the rat rostral ventrolateral medulla: relationship to sympathetic nerve activity and the C1 adrenergic cell group. *J Neurosci* 8: 1286–1301, 1988.
38. **Nishi EE, Bergamaschi CT, Oliveira-Sales EB, Simon KA, Campos RR.** Losartan reduces oxidative stress within the rostral ventrolateral medulla of rats with renovascular hypertension. *Am J Hypertens* 26: 858–865, 2013.
39. **Osborn JW, Fink GD, Kuroki MT.** Neural mechanisms of angiotensin II-salt hypertension: implications for therapies targeting neural control of the splanchnic circulation. *Curr Hypertens Rep* 13: 221–228, 2011.
40. **Osborn JW, Fink GD, Sved AF, Toney GM, Raizada MK.** Circulating angiotensin II and dietary salt: converging signals for neurogenic hypertension. *Curr Hypertens Rep* 9: 228–235, 2007.
41. **Osborn JW, Hendel MD, Collister JP, Ariza-Guzman PA, Fink GD.** The role of the subfornical organ in angiotensin II-salt hypertension in the rat. *Exp Physiol* 97: 80–88, 2012.
42. **Pawloski-Dahm CM, Gordon FJ.** Increased dietary salt sensitizes vasomotor neurons of the rostral ventrolateral medulla. *Hypertension* 22: 929–933, 1993.
43. **Ployngam T, Collister JP.** An intact median preoptic nucleus is necessary for chronic angiotensin II-induced hypertension. *Brain Res* 1162: 69–75, 2007.
44. **Ployngam T, Collister JP.** Role of the median preoptic nucleus in chronic angiotensin II-induced hypertension. *Brain Res* 1238: 75–84, 2008.
45. **Porter JP, Brody MJ.** Spinal vasopressin mechanisms of cardiovascular regulation. *Am J Physiol Regul Integr Comp Physiol* 251: R510–R517, 1986.
46. **Potts PD, Hirooka Y, Dampney RA.** Activation of brain neurons by circulating angiotensin II: direct effects and baroreceptor-mediated secondary effects. *Neuroscience* 90: 581–594, 1999.
47. **Pyner S, Coote JH.** Identification of branching paraventricular neurons of the hypothalamus that project to the rostroventrolateral medulla and spinal cord. *Neuroscience* 100: 549–556, 2000.
48. **Rathner JA, McAllen RM.** Differential control of sympathetic drive to the rat tail artery and kidney by medullary premotor cell groups. *Brain Res* 834: 196–199, 1999.
49. **Sakima A, Yamazato M, Sesoko S, Muratani H, Fukiyama K.** Cardiovascular and sympathetic effects of L-glutamate and glycine injected into the rostral ventrolateral medulla of conscious rats. *Hypertens Res* 23: 633–641, 2000.
50. **Scheuer DA, Zhang J, Toney GM, Mifflin SW.** Temporal processing of aortic nerve evoked activity in the nucleus of the solitary tract. *J Neurophysiol* 76: 3750–3757, 1996.
51. **Schlaich MP, Lambert E, Kaye DM, Krozowski Z, Campbell DJ, Lambert G, Hastings J, Aggarwal A, Esler MD.** Sympathetic augmentation in hypertension: role of nerve firing, norepinephrine reuptake, and angiotensin neuromodulation. *Hypertension* 43: 169–175, 2004.
52. **Schramm LP, Strack AM, Platt KB, Loewy AD.** Peripheral and central pathways regulating the kidney: a study using pseudorabies virus. *Brain Res* 616: 251–262, 1993.
53. **Schreihofer AM, Guyenet PG.** Identification of C1 presympathetic neurons in rat rostral ventrolateral medulla by juxtacellular labeling in vivo. *J Comp Neurol* 387: 524–536, 1997.
54. **Shafton AD, Ryan A, Badoer E.** Neurons in the hypothalamic paraventricular nucleus send collaterals to the spinal cord and to the rostral ventrolateral medulla in the rat. *Brain Res* 801: 239–243, 1998.
55. **Shi L, Yao J, Stewart L, Xu Z.** Brain C-FOS expression and pressor responses after iv or icv angiotensin in the near-term ovine fetus. *Neuroscience* 126: 979–987, 2004.
56. **Shi P, Stocker SD, Toney GM.** Organum vasculosum laminae terminalis contributes to increased sympathetic nerve activity induced by central hyperosmolality. *Am J Physiol Regul Integr Comp Physiol* 293: R2279–R2289, 2007.
57. **Smithwick RH, Thompson JE.** Splanchnicectomy for essential hypertension; results in 1,266 cases. *J Am Med Assoc* 152: 1501–1504, 1953.
58. **Stein RD, Weaver LC, Yardley CP.** Ventrolateral medullary neurones: effects on magnitude and rhythm of discharge of mesenteric and renal nerves in cats. *J Physiol* 408: 571–586, 1989.
59. **Stocker SD, Meador R, Adams JM.** Neurons of the rostral ventrolateral medulla contribute to obesity-induced hypertension in rats. *Hypertension* 49: 640–646, 2007.
60. **Stocker SD, Simmons JR, Stornetta RL, Toney GM, Guyenet PG.** Water deprivation activates a glutamatergic projection from the hypothalamic paraventricular nucleus to the rostral ventrolateral medulla. *J Comp Neurol* 494: 673–685, 2006.
61. **Stocker SD, Toney GM.** Median preoptic neurones projecting to the hypothalamic paraventricular nucleus respond to osmotic, circulating Ang II and baroreceptor input in the rat. *J Physiol* 568: 599–615, 2005.
62. **Strack AM, Sawyer WB, Hughes JH, Platt KB, Loewy AD.** A general pattern of CNS innervation of the sympathetic outflow demonstrated by transneuronal pseudorabies viral infections. *Brain Res* 491: 156–162, 1989.
63. **Strack AM, Sawyer WB, Platt KB, Loewy AD.** CNS cell groups regulating the sympathetic outflow to adrenal gland as revealed by transneuronal cell body labeling with pseudorabies virus. *Brain Res* 491: 274–296, 1989.
64. **Sun MK, Guyenet PG.** Medullospinal sympathoexcitatory neurons in normotensive and spontaneously hypertensive rats. *Am J Physiol Regul Integr Comp Physiol* 250: R910–R917, 1986.
65. **Tagawa T, Dampney RA.** AT_1 receptors mediate excitatory inputs to rostral ventrolateral medulla pressor neurons from hypothalamus. *Hypertension* 34: 1301–1307, 1999.
66. **Tanaka J, Kaba H, Saito H, Seto K.** Subfornical organ neurons with efferent projections to the hypothalamic paraventricular nucleus: an electrophysiological study in the rat. *Brain Res* 346: 151–154, 1985.
67. **Toney GM, Daws LC.** Juxtacellular labeling and chemical phenotyping of extracellularly recorded neurons in vivo. *Methods Mol Biol* 337: 127–137, 2006.
68. **Toney GM, Pedrino GR, Fink GD, Osborn JW.** Does enhanced respiratory-sympathetic coupling contribute to peripheral neural mechanisms of angiotensin II-salt hypertension? *Exp Physiol* 95: 587–594, 2010.
69. **Whitworth JA.** 2003 World Health Organization (WHO)/International Society of Hypertension (ISH) statement on management of hypertension. *J Hypertens* 21: 1983–1992, 2003.
70. **Yoshimoto M, Miki K, Fink GD, King A, Osborn JW.** Chronic angiotensin II infusion causes differential responses in regional sympathetic nerve activity in rats. *Hypertension* 55: 644–651, 2010.